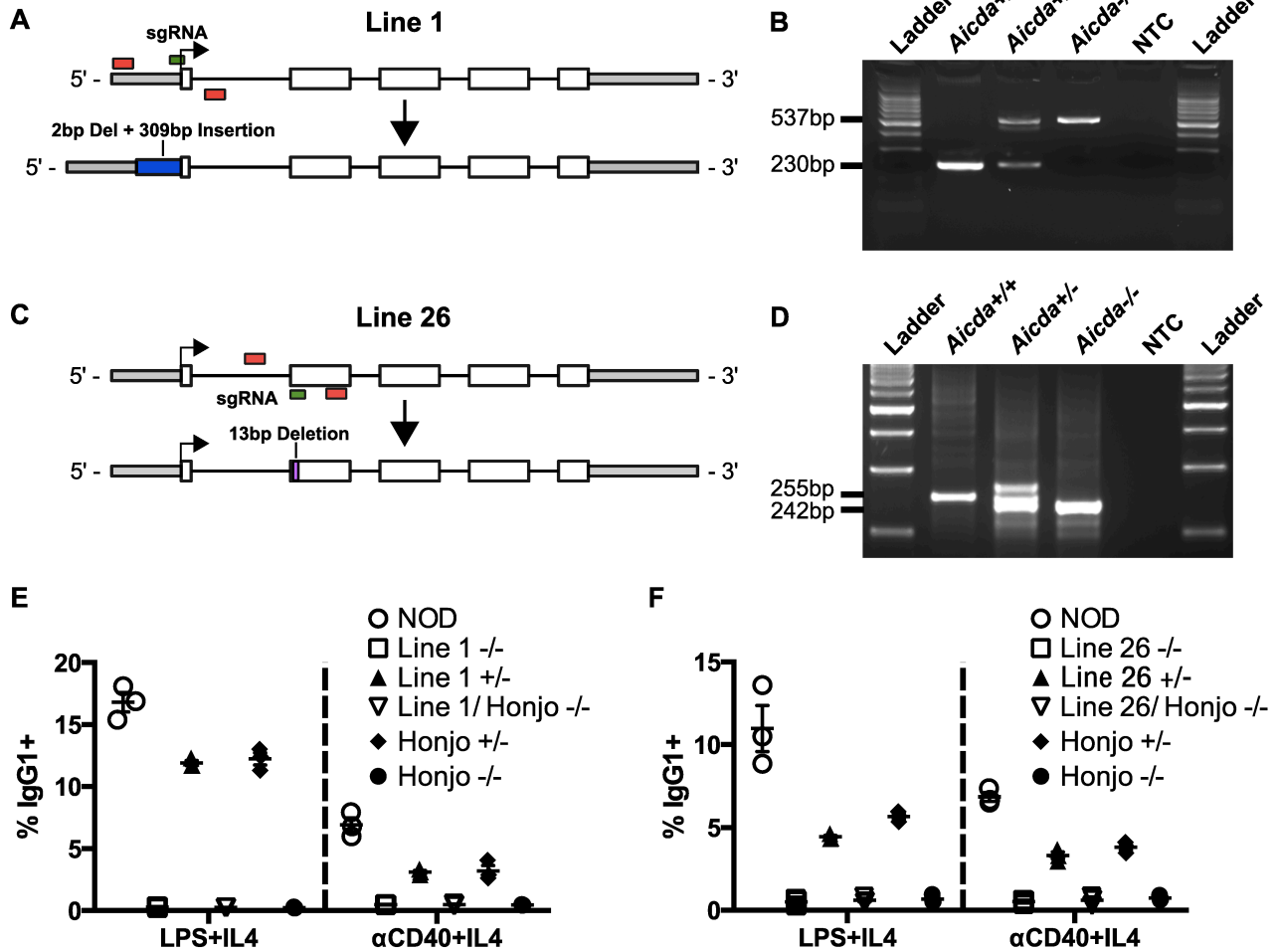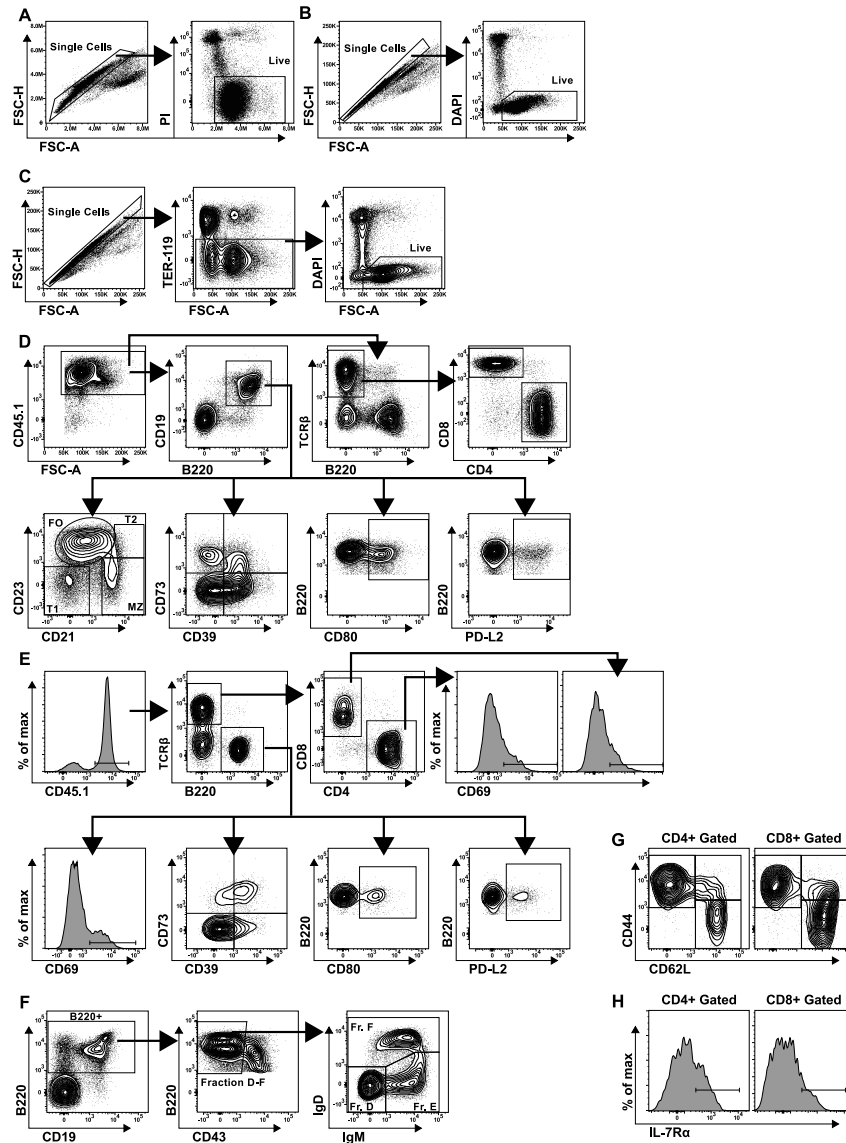**Supplementary Figure 1: CRISPR/Cas9-mediated generation and verification of *Aicda-/-* NOD mice.** (A) Schematic diagram depicting *Aicda* gene structure and the locations of genotyping primers (red) and sgRNA (green) complementary sequences and 2bp deletion with 309bp insertion generated (blue) for NOD.*Aicda*$^{-/-}$ Line 1. (B) Representative image of genotyping for NOD.*Aicda*$^{-/-}$ Line 1. (C) Structure of *Aicda* and the locations of genotyping primers (red) and sgRNA (green) complementary sequences and 13bp deletion generated (pink) for NOD.*Aicda*$^{-/-}$ Line 26. (D) Representative image of genotyping for NOD.*Aicda*$^{-/-}$ Line 26. (E-F) Splenic B-lymphocytes purified from F1 offspring of NOD.*Aicda*$^{-/-}$ X B6.*Aicda*$^{-/-}$ (n=3 per genotype) were cultured for 96 hours under stimulation by murine IL-4 (25 ng/mL) and LPS (50 μg/mL) or anti-CD40 (1 μg/mL) for 96 hours then analyzed for isotype switching to IgG1 by flow cytometry for Line 1 (E) and Line 26 (F). Mann-Whitney analysis was used to calculate *p*-values. All scatter plots show Mean±SEM.
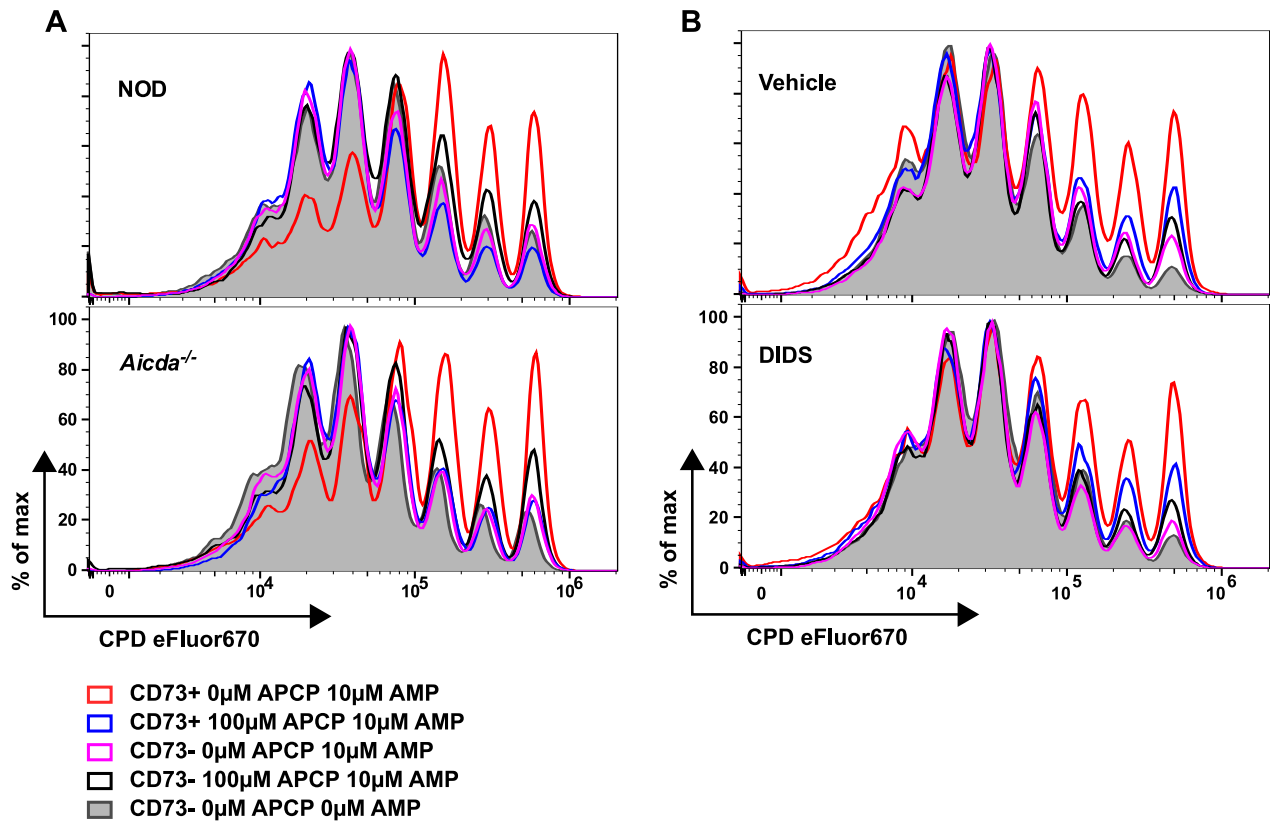
Supplementary Figure 2: Flow cytometry gating strategies for identification of lymphocyte populations.
Representative live cell gating using propidium iodide (PI, A) or DAPI (B) as a marker to exclude dead cells. Non-singlets are excluded as shown FSC-H vs FSC-A. Singlets are then shown PI or DAPI vs FSC-A and PI$^-$ or DAPI$^-$ cells are gated. (C) Representative live cell gating for spleen and PLN analysis of DIDS-treated mice. First, non-singlets are excluded as shown FSC-H vs FSC-A, then TER119$^-$ and DAPI$^-$ cells are gated as shown. (D) Representative gating strategy used to identify spleen and PLN T-cell and B-lymphocyte subsets was performed as follows: live singlets were first gated on CD45.1$^+$ to eliminate any non-leukocyte cells then B220$^+$ CD19$^+$ B-lymphocytes and TCRβ$^+$ B220$^-$ T-cells were gated as shown. CD4$^+$ and CD8$^+$ T-cell subsets were gated as shown. Splenic T1 (CD21$^-$ CD23$^-$), T2 (CD21^{hi} CD23$^+$), Follicular (CD21$^+$ CD23$^+$) and Marginal Zone (CD21^{hi} CD23$^-$) B-lymphocyte subsets were gated as shown. Spleen and PLN CD73$^+$ CD39$^-$, CD73$^+$ CD39$^+$ and CD73$^-$ CD39$^-$, CD80$^+$ and PD-L2$^+$ B-lymphocyte populations were gated as shown. (E) Representative gating strategy used to identify islet-infiltrating T-cell and B-lymphocyte populations was performed as follows: live singlets were first gated on CD45.1$^+$ to eliminate any non-leukocyte cells then B220$^+$ TCRβ$^-$ B-lymphocytes and TCRβ$^+$ B220$^-$ T-cells were gated as shown. CD4$^+$ and CD8$^+$ T-cell CD69 and IL-7Rα subsets were gated as shown. Among B-lymphocytes, CD69$^+$, CD73$^+$ CD39$^-$, CD73$^+$ CD39$^+$ and CD73$^-$ CD39$^-$, CD80$^+$ and PD-L2$^+$ populations were gated as shown. (F) Representative gating strategy used to identify BM B-lymphocyte populations as follows: B220$^+$ cells are gated and further stratified for an absence of CD43 expression. Gated CD43$^-$ cells are shown as IgD vs IgM, and divided amongst Hardy Fractions D (IgM$^-$ IgD$^-$), E (IgM$^+$ IgD$^{-/low}$), or F (IgM$^{+/low}$ IgD$^+$). (G-H) Representative gating strategy used to identify naïve (CD44$^-$ CD62L^{hi}), effector (Eff, CD44$^+$ CD62L$^-$) central memory (CM, CD44$^+$ CD62L^{hi}) subsets (G) and IL-7Rα$^+$ (H) islet-infiltrating CD4$^+$ and CD8$^+$ T-cells.
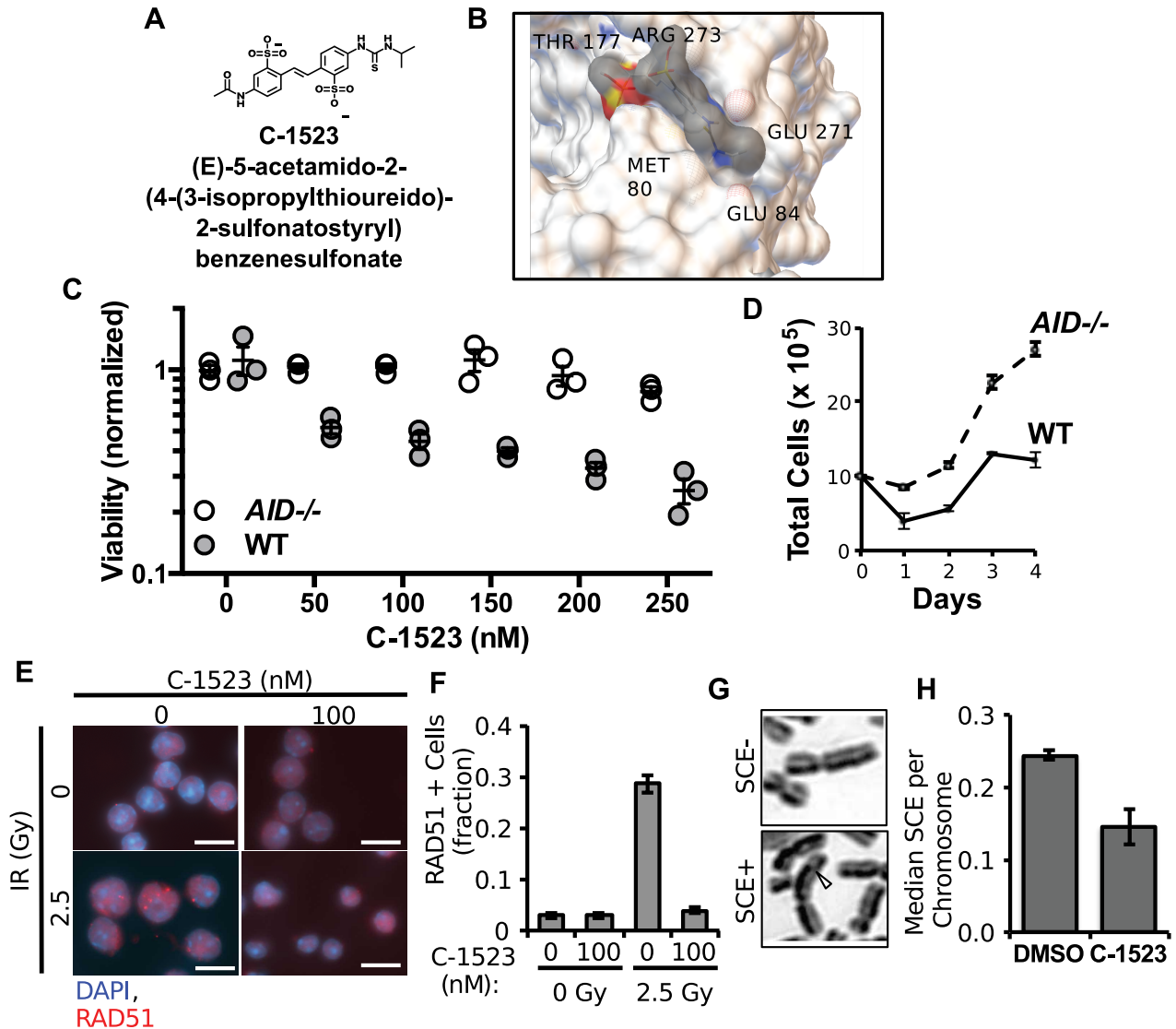
Supplementary Figure 3

Supplementary Figure 3: CD73+ B-lymphocytes suppress T-cell proliferation.
(A) Representative flow cytometric histograms of 1.0×10^5 CD73-depleted purified CD4$^+$ T-cells from 7-10 week-old male NOD mice labeled with Cell Proliferation Dye eFluor670 (CPD) and co-cultured for 4 days with 1.0×10^5 CD73$^+$ or CD73$^-$ B-lymphocytes from pooled spleens of 7-10 week old male NOD (n=6 biological replicates) or NOD.*Aicda$^{-/-}$* (n=10 biological replicates) mice under stimulation conditions consisting of soluble anti-CD40 (1 µg/mL), plate-bound anti-CD3ε (5 µg/mL) and soluble anti-CD28 (2 µg/mL) with 0 (baseline) or 10 µM AMP in the presence or absence of 100 µM APCP. (B) Representative flow cytometric histograms of 1.0×10^5 CD73$^-$ NOD T-cells labeled with Cell Proliferation Dye (CPD) eFluor670 and co-cultured for 4 days with 1.0×10^5 CD73$^+$ or CD73$^-$ B-lymphocytes from pooled spleens of vehicle (n=6 biological replicates) or DIDS treated (n=6 biological replicates) mice under stimulation conditions consisting of soluble anti-CD40 (1 µg/mL), plate-bound anti-CD3ε (5 µg/mL) and soluble anti-CD28 (2 µg/mL) with 0 (baseline) or 10 µM AMP in the presence or absence of 100 µM APCP.

Supplementary Figure 4

A

C-1523
(E)-5-acetamido-2-
(4-(3-isopropylthioureido)-
2-sulfonatostyryl)
benzenesulfonate

B

C

D

E

F

G

H

Supplementary Figure 4: C-1523 inhibits RAD51 dependent homologous recombination. (A) Chemical structure of C-1523, a derivative of DIDS. (B) Model of C-1523 binding to RAD51 monomer (1SZP) indicating the associated amino acid residues. The RAD51 structure was obtained from the Protein Data Bank (PDB) using the pdb code 1SZP. Only Chain A was used in the docking analysis. (C) WT and B6.*Aicda*^{-/-} purified B-cells were incubated with αCD40/IL-4 and with increasing dose of C-1523. Cells were counted via Trypan Blue exclusion test and normalized to vehicle (0 nM). (D) Graph showing total number of WT and B6.*Aicda*^{-/-} purified B-cells at 100nM dose over a period of 4 days. (E) Representative images of RAD51 foci in primary cells. (F) Quantification of RAD51 by immunofluorescence in purified activated primary mouse B cells 24 h after 0 or 2.5 Gy IR and treatment with C-1523 (100 nM) or vehicle. (G) Representative images of metaphases from HEK293T-cells showing a positive sister chromatid exchange (SCE+) and an individual chromosome with no exchange (SCE-). A white arrow indicates the location of the exchange. HEK293T-cells were cultured with either vehicle (DMSO) or 100 nM C-1523 for three days. Cells were then incubated with 10 µM BrdU for 44 hours. Colcemid was added to cultures for 30 min to 1 hour to induce metaphase arrest. After methanol/acetic acid fixation, slides were stained with Hoescht, exposed to UV, and then stained with Giemsa. Metaphase chromosomes were visualized by bright-field microscopy, and 20 metaphases were scored per sample. (H) Quantification of sister chromatid exchange observed in the metaphases of HEK293T-cells treated either with vehicle or 100nM C-1523. Twenty metaphases from three individual experiments were scored for each treatment.